

***c*-axis charge distribution in stage-3 and -4 graphite acceptor compounds**

R. S. Markiewicz

*Department of Physics, Northeastern University, Boston, Massachusetts 02115*

(Received 10 August 1983)

By generalizing the acceptor model previously developed for stage-2 graphite intercalation compounds, we show that the principal Fermi surfaces of stage-3 and -4 compounds can be described in terms of a single extra parameter. This parameter is directly related to *c*-axis screening of the intercalant layer potential, and can be used to determine how much charge is transferred to the interior layers. We find that the interior-layer charge transfer is similar for all intercalants and stages. Screening effects, while substantial, are weaker than most theoretical predictions.

We have recently shown<sup>1-3</sup> that the principal Fermi surfaces of all stage-2 graphite acceptor compounds can be described in a unified manner: The bands are just those of an isolated system of two graphite layers, calculated analogously to the Slonczewski-Weiss-McClure (SWM) model<sup>4</sup> for three-dimensional (3D) graphite, and with the *same* band parameters as found in bulk graphite. The intercalant layer acts only to provide a charge transfer *f*; measured values of *f* are in good agreement with earlier determinations.<sup>2</sup> The secondary structure observed in de Haas-van Alphen and related measurements can then be understood in terms of magnetic interaction,<sup>2,5</sup> magnetic interferometer effects,<sup>3</sup> and superlattice effects.<sup>6</sup>

In this paper, we extend this model to stages 3 and 4, and

compare the results with existing data. In these higher stages, the intercalant plays an extra role: Holes are attracted to the graphite layers which bound the intercalant layer to screen the ionic charges. Calculations of this effect<sup>7-10</sup> have suggested that the screening is nearly complete in that the fraction of holes, *f<sub>i</sub>*, which is on each interior graphite layer (i.e., a layer not adjacent to an intercalant layer) is approximately zero. (For a *uniform* charge distribution, *f<sub>i</sub>* is  $\frac{1}{3}$  or  $\frac{1}{4}$  in stage 3 or 4, respectively.)

To include screening effects, we introduce a single extra parameter  $\mu_0$ , which measures how strongly holes are attracted to the boundary layer. For stage 3, there are three interacting graphite bands, and the SWM construction gives the energy bands as solutions of the  $6 \times 6$  matrix:

$$\det \begin{pmatrix} \Delta - E - \mu_0 & -\gamma_0 \sigma^* & -\gamma_1 & \gamma_4 \sigma & \gamma_5/2 & 0 \\ -\gamma_0 \sigma & -E - \mu_0 & -\gamma_4 \sigma & \gamma_3 \sigma^* & 0 & \gamma_2/2 \\ -\gamma_1 & -\gamma_4 \sigma^* & \Delta - E & \gamma_0 \sigma & -\gamma_1 & -\gamma_4 \sigma^* \\ \gamma_4 \sigma^* & \gamma_3 \sigma & \gamma_0 \sigma^* & -E & \gamma_4 \sigma^* & \gamma_3 \sigma \\ \gamma_5/2 & 0 & -\gamma_1 & \gamma_4 \sigma & \Delta - E - \mu_0 & -\gamma_0 \sigma^* \\ 0 & \gamma_2/2 & -\gamma_4 \sigma & \gamma_3 \sigma^* & -\gamma_0 \sigma & -E - \mu_0 \end{pmatrix} = 0. \quad (1)$$

Here  $\sigma$  and the band parameters  $\gamma_i$  have their standard definitions<sup>1,11</sup> while  $\Delta = \bar{\Delta} - \gamma_2 + \gamma_5$ , where  $\bar{\Delta}$  is the 3D value of Ref. 11. The values of the band parameters are taken to be the same as in stage 2,<sup>2</sup> with  $\gamma_2$  and  $\gamma_5$  taking their bulk values.<sup>11</sup> The matrix (1) can be reduced to a  $2 \times 2$  matrix, with eigenfunctions on the bounding layers only, and a  $4 \times 4$ , which mixes bounding and interior eigenfunctions. These remaining matrices are then solved numerically to find the Fermi surfaces.

The above model is similar to a number of models which have appeared recently in the literature.<sup>12-15</sup> It is nearly identical to the model of Leung and Dresselhaus,<sup>12</sup> (LD), except that these authors included a *c*-axis dispersion due to a sandwich-sandwich interaction. Shayegan, Dresselhaus, and Dresselhaus<sup>13</sup> applied this model to donor intercalation compounds, but took  $\mu_0 = 0$ . Holzwarth<sup>14</sup> developed a single sandwich model, also with  $\mu_0 = 0$ . Blinowski and Rigaux<sup>15</sup> (BR) included nonzero  $\mu_0$  (in their notation,  $\mu_0 \rightarrow 2\delta$ ) but simplified the graphite band structure, retaining only  $\gamma_0$ ,  $\gamma_1$ , and  $\Delta$ . This leads to incorrect values for  $\gamma_0$  and  $\gamma_1$  derived from experimental Fermi surfaces (compare Refs. 1 and 16).

The significance of  $\mu_0$  can most easily be seen by setting all parameters to zero except  $\gamma_0$  and  $\mu_0$ . In this case, the three layers decouple, and the three bands are cones ( $E \propto k$ ). The interior band is raised (or lowered) with respect to the other two bands by the energy  $\mu_0$ . Hence, if  $\mu_0 = -E_F$ , the interior band is unpopulated, while if  $\mu_0 > -E_F$ , the interior band contains electrons, not holes. When  $\gamma_1$  is not zero, it is still true that if  $\mu_0 = -E_F$ , one band is depopulated. However, this band is no longer strictly associated with interior layer holes:  $\gamma_1$  mixes holes on different layers, so  $f_i > 0$ . To make  $f_i = 0$ , it is necessary for  $\mu_0 > -E_F$ . Then, of the three Fermi surfaces, one would be electronlike, and the interior layer would be semimetallic, with equal numbers of electrons and holes (just as in bulk graphite). It is not clear to what extent these band-structure complications were taken into account in calculations of screening effects.<sup>7-10</sup> Nevertheless, we do not find good agreement between theory and experiment assuming  $f_i = 0$ , unless the band parameters are very different from those of bulk graphite. Instead, we find that all three Fermi surfaces are holelike, and  $f_i > 0$ .

Figure 1 shows our analysis for stage-3 AsF<sub>5</sub>-graphite.<sup>16</sup>

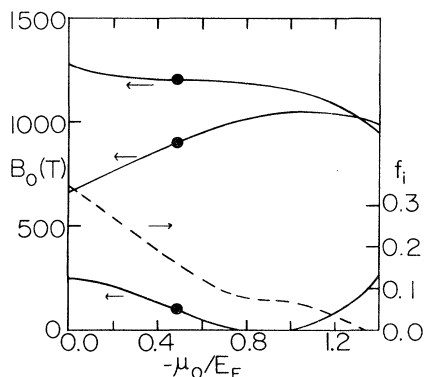


FIG. 1. Calculated value of Fermi-surface areas (expressed as de Haas-van Alphen oscillation frequencies) for stage-3  $\text{AsF}_5$ -graphite compounds as the screening parameter  $\mu_0$  is varied. ●: data of Ref. 16. Dashed line:  $f_i$ .

Three principal surfaces are found in Shubnikov-de Haas measurements; since the secondary frequencies are second and third harmonics of the lowest principal frequency, there is no ambiguity in this selection. The sum of the three surface areas gives the charge transfer  $f$  (if one surface is electronlike, its area should be subtracted). For the observed value of  $f$ , Fig. 1 shows how the areas of the Fermi surfaces change as  $\mu_0$  is varied, along with the experimental values of Ref. 16. Figure 1 also plots an approximate value of  $f_i$ —we take  $f_i$  as the probability that a hole at the Fermi level will be found on a particular interior layer. When  $f_i \approx 0$ , the two larger Fermi surfaces have nearly the same cross-sectional areas, contrary to experiment. The best fit to the Fermi surface areas gives  $f_i = 0.16$ , close to the value found in Ref. 16 based on the BR model. A similar analysis was carried out for samples of  $\text{SbCl}_5$ - and  $\text{HNO}_3$ -graphite, and the resulting values of  $f$ ,  $f_i$ , and  $\delta$  are listed in Table I, along with values of  $f$  for stage-2 samples.

These calculations were repeated for stage-4 samples, and

the results are also listed in Table I. For this case, the  $8 \times 8$  matrix is reduced to two  $4 \times 4$  matrices by neglecting some small terms involving trigonal warping ( $\gamma_3$ ). From Table I it can be seen that the charge transfer  $f$  is nearly the same for all stages of a given intercalant. (The value of  $f$  for stage-4  $\text{AsF}_5$ -graphite seems low, although not lower than values observed in partially deintercalated samples of stage 2.<sup>1</sup> However, it may be that the largest Fermi surface of the stage-4 sample was not observed due to too large a scattering rate, thereby invalidating the present analysis.)

From Table I it can be seen that the value of  $f_i$ , or  $\mu_0/E_F$ , is similar for all intercalants and for both stages 3 and 4. Hence it is possible to draw a single curve of Fermi-surface areas versus  $f$  for either stage 3 or stage 4, which gives good agreement with the observed areas. Figure 2 shows the data used in Table I plotted assuming  $\mu_0/(-E_F) = 0.48$  for all samples.

There seems to be a trend for  $f_i$  to increase as  $f$  decreases (Fig. 3). While theoretical predictions<sup>7-10</sup> show this trend, they generally underestimate the values of  $f_i$ . As Fig. 3 shows, the earliest calculation<sup>7</sup> comes closest to describing the data, while more recent calculations<sup>9,10</sup> predict considerably smaller values. The explanation of this discrepancy may be found in a recent calculation for a stage-3 donor (Li) compound.<sup>17</sup> It was found that the *total* electronic distribution is very nonuniform, due principally to polarization effects, but the conduction electron distribution is much more spatially uniform.

It is interesting to note that the graphite acceptor compounds form an almost ideal system of 2D synthetic metals: The overall band structure is completely known in terms of graphite band parameters, and any superlattice effects must be consistent with these values. Within a given stage the carrier concentration can be varied over a wide range by varying the intercalant, or with some compounds, by partial deintercalation.<sup>1</sup>

A final comment: The difference between our model and that of LD<sup>12</sup> may be an appropriate distinction between donor and acceptor compounds. In donor compounds, the thickness of the intercalant layer is comparable with that of the graphite layer, while the carbon atoms stack in  $A/A$

TABLE I. Charge transfer and interior layer fraction for acceptor compounds.

| Material<br>$X(s)$    | Stage<br>$n$ | Charge<br>transfer<br>$f$ | $C_{ns}X$                               |                               | Source<br>of data<br>Reference |
|-----------------------|--------------|---------------------------|---|-------------------------------|--------------------------------|
|                       |              |                           | Screening<br>function<br>$\mu_0/(-E_F)$ | Interior<br>fraction<br>$f_i$ |                                |
| $\text{AsF}_5(8)$     | 2            | 0.4–0.46                  |   |                               | 1                              |
|                       | 3            | 0.445                     | 0.49                                    | 0.16                          | 1                              |
|                       | 4            | 0.34                      | 0.45                                    | 0.17                          | 18                             |
| $\text{SbCl}_5(14)$   | 2            | 0.51, 0.57                |   |                               | 2, 19                          |
|                       | 3            | 0.57                      | 0.45                                    | 0.18                          | 19                             |
|                       | 4            | 0.66                      | 0.45                                    | 0.17                          | 19                             |
| $\text{HNO}_3(8)$     | 3            | 0.29                      | 0.4                                     | 0.20                          | 19                             |
|                       | 2            | 0.19                      |   |                               | 20                             |
| (Residue<br>compound) | 3            | 0.23                      | 0.3                                     | 0.24                          | 20                             |
|                       | 4            | 0.267                     | 0.6                                     | 0.14                          | 20                             |

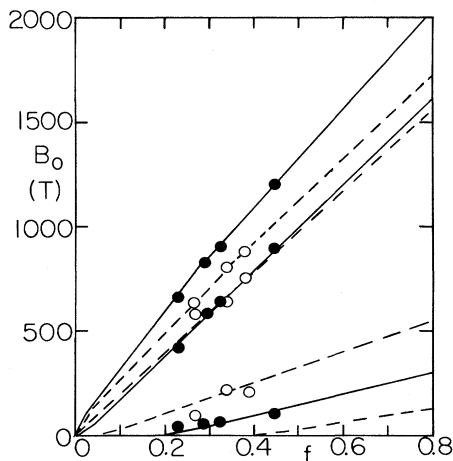


FIG. 2. Fermi-surface areas plotted vs charge transfer, assuming  $-\mu_0/E_F=0.48$ . Lines: theory; circles: data of Table I (with  $f$  scaled to a  $C_{8n}X$  compound). Stage 3: —, ●; stage 4: ---, ○.

fashion across the intercalant layer. Hence LD model the intercalation compound by 3D graphite with one missing graphite layer representing each intercalant layer—the  $c$ -axis dispersion is due to the coupling of carbon layers across this gap due to  $\gamma_2$  and  $\gamma_5$ . In an acceptor compound the intercalant layer is thicker, and the stacking of carbon layers

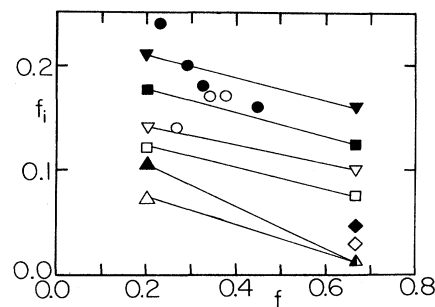


FIG. 3. Interior layer fraction  $f_i$  vs charge transfer (adjusted to a  $C_{8n}X$  compound). Open symbols: stage 3; filled symbols: stage 4. ○, ●: data of Table I. ▽, ▼: theory of Ref. 7. □, ■: Ref. 8. ◇, ◆: Ref. 9. △, ▲, ▲: Ref. 10. Straight lines are guides to the eye.

across the intercalant is usually  $A/B$  ( $AsF_5$ ,  $SbCl_5$ ). Hence a more appropriate model would be to remove *two* graphite layers for each intercalant layer. But this completely decouples separate sandwiches, since the SWM model does not include any interaction of carbon atoms more than two layers apart.

#### ACKNOWLEDGMENTS

This research is supported by AFOSR under Contract No. F49620-82-C-0076.

- <sup>1</sup>R. S. Markiewicz, *Solid State Commun.* **44**, 791 (1982).
- <sup>2</sup>R. S. Markiewicz, C. Lopatin, and C. Zahopoulos, in *Intercalated Graphite*, proceedings of the Materials Research Society Symposium, Vol. 20, edited by M. S. Dresselhaus, G. Dresselhaus, J. E. Fischer, and M. J. Moran (North-Holland, New York, 1983), p. 135.
- <sup>3</sup>R. S. Markiewicz and C. Zahopoulos, *Phys. Rev. B* **27**, 7820 (1983).
- <sup>4</sup>J. C. Slonczewski and P. R. Weiss, *Phys. Rev.* **99**, A636 (1955); J. W. McClure, *Phys. Rev.* **108**, 612 (1957).
- <sup>5</sup>D. Shoenberg, *Can. J. Phys.* **46**, 1915 (1968).
- <sup>6</sup>S. Tanuma, O. Takahashi, and Y. Iye, in *Physics of Intercalations Compounds*, edited by L. Pietronero and E. Tosatti (Springer, Berlin, 1981), p. 90.
- <sup>7</sup>L. Pietronero, S. Strässler, H. R. Zeller, and M. J. Rice, *Phys. Rev. Lett.* **41**, 763 (1978).
- <sup>8</sup>S. A. Safran and D. R. Hamann, *Phys. Rev. B* **23**, 565 (1981).
- <sup>9</sup>S. Shimamura and A. Morita, *J. Phys. Soc. Jpn.* **51**, 502 (1982).

- <sup>10</sup>T. Ohno and H. Kamimura, *J. Phys. Soc. Jpn.* **52**, 223 (1983).
- <sup>11</sup>L. G. Johnson and G. Dresselhaus, *Phys. Rev. B* **7**, 2275 (1973).
- <sup>12</sup>S. Y. Leung and G. Dresselhaus, *Phys. Rev. B* **24**, 3490 (1981).
- <sup>13</sup>M. Shayegan, M. S. Dresselhaus, and G. Dresselhaus, *Phys. Rev. B* **25**, 4157 (1982).
- <sup>14</sup>N. A. W. Holzwarth, *Phys. Rev. B* **21**, 3665 (1980).
- <sup>15</sup>J. Blinowski and C. Rigaux, *J. Phys. (Paris)* **41**, 667 (1980).
- <sup>16</sup>R. S. Markiewicz, H. R. Hart, Jr., L. V. Interrante, and J. S. Kasper, *Synth. Met.* **2**, 331 (1980).
- <sup>17</sup>N. A. W. Holzwarth, S. G. Louie, and S. Rabii, *Phys. Rev. B* **28**, 1013 (1983).
- <sup>18</sup>Y. Iye, O. Takahashi, and S. Tanuma, *Solid State Commun.* **33**, 1071 (1980).
- <sup>19</sup>O. Takahashi, Y. Iye, and S. Tanuma, *Solid State Commun.* **37**, 866 (1981).
- <sup>20</sup>F. Battallan, I. Rosenman, and C. Simon, *Synth. Met.* **2**, 353 (1980).